Abstract

Contents

1 Introduction **5**
- 1.1 Quantum Computing . . . 5
- 1.2 Quantum Error Correction . . . 5
- 1.3 Weakly coupled carbons; a naturally occurring register . . . 5

2 Electronic spins in Diamond **7**
- 2.1 Spin Control . . . 7

3 Weakly-coupled Carbon Spins **9**
- 3.1 Addressing weakly-coupled carbons trough dynamical decoupling . . . 9
- 3.2 Characterizing the Nuclear-spin environment . . . 10
- 3.3 Controlling weakly coupled carbons trough the electronic spin . . . 12
- 3.4 Carbon Initialization & Readout . . . 12

4 Deterministic Parity Measurements **13**
- 4.1 Entanglement . . . 13
- 4.2 Verification of Entanglement . . . 13

5 Outlook: towards Quantum Error Correction **15**

A State Initialization **19**

B Bell State Tomography **21**

C Entanglement wittness **23**

D Simulations **25**

1 Introduction

1.1 Quantum Computing

The idea of using a quantum mechanical system to simulate physics was first explored by Feynman[5]. Because the Hilbert space(/state space?) of a quantum mechanical system scales exponentially with it's size one would need an exponentially large classical computer to simulate it's behavior. By manipulating a quantum mechanical system directly this scaling problem can be circumvented.

It was quantum simulation that eventually led to the idea of exploiting quantum effects to perform more efficient calculations but it wasn't until Shor's discovery of a remarkably efficient quantum algorithm for prime factorization in 1994[9] that quantum information science really took off.

Shor's algorithm was the first example where a quantum computer can provide an exponential speedup over a classical computer. Shor's and other quantum algorithms allow solving classes of problems that were previously unsolvable, a well known example being the breaking of classical encryption codes.

By now Shor's algorithm has been shown to work on a range of different small scale quantum computers [13] [Needs reference to Shor in different systems or basic algorithms in range of systems] but making a scalable quantum computer that can take full advantage of the exponential speedup proves elusive.

1.2 Quantum Error Correction

1.3 Weakly coupled carbons; a naturally occurring register

The Nitrogen Vacancy centre in diamond is a well investigated system[4] and a promising candidate for quantum computation[2]. In order to implement three qubit measurement based QEC we need three qubits plus ancillae that we can initialise, measure and conditionally perform operations on. These extra qubits are found in Carbon–13 atoms, which are normally a source of decoherence. These atoms can be addressed using a resonant decoupling sequence[10].

2 Electronic spins in Diamond

It has been shown that the nuclear- and electron- spin-state of the NV- center can be initialized, coherently controlled and read-out using microwave- and laser- pulses[8]. In these experiments two lasers that are resonant with transitions in the NV- center are used to initialize the electronic spin state. One of these two lasers is used to read out the electronic spin state and an off-resonant laser is used to reset the system. Microwaves are used to drive transitions between the different nuclear and electronic spin states.

Strongly coupled nuclear spins can be initialized by conditionally rotating the electronic state to a state that is read out only if the Carbon is in the desired state, when the electronic state readout has a positive result the system is projected into the desired state. We call this Measurement Based Initialization (MBI). Our experiments are build around the same basic tools. Each experiment starts with a Charge-Resonance check that verifies if the lasers are still on resonance. After that the Nitrogen spin state is initialized using MBI. Once the system is initialized our actual experiment is performed. This consists of microwave pulses and a single or multiple readouts.

All experiments were performed on a custom-build cryostat setup operating at liquid helium temperatures described in detail in Bernien [1, chap. 3]. The setup was additionally outfitted with a movable neodymium magnet that applied a magnetic field of 300G to the sample.

2.1 Spin Control

The electronic ground state Hamiltonian can be written as[7]:

$$H_{GS} = \Delta {S_z}^2 + \gamma_e \mathbf{B} \cdot \mathbf{S} \tag{2.1}$$

With zero field splitting $\Delta \approx 2.88$GHz and gyro-magnetic ratio $\gamma_e = 2.802$ MHz/G . In this expression the interactions with the Nitrogen nucleus and the Carbon spin bath are not included. By applying a magnetic field B_z a long the NV axis the degeneracy of the $m_s = \pm 1$ states is lifted by the Zeeman effect. We define our electronic qubit by the two level system with $m_s = 0 := |0\rangle$ and $m_s = +1 := |1\rangle$.

On the Bloch-sphere the state vector rotates around the quantization axis with a frequency depending on the energy splitting of the two states given by the Larmor frequency $\omega_L = \Delta - \gamma_e B_z$.[1] By applying an external field a term is effectively added to the Hamiltonian, changing the quantization axis and thereby its evolution. By applying microwaves with the right frequency this can be used to selectively drive the transition from the $|0\rangle$ state to the $|1\rangle$stateJelezko et al. [6].

[1] When ω_L is used as a vector it is pointing in the $\hat{z}$ direction.

3

Weakly-coupled Carbon Spins

Similar to how the electronic spin state can be controlled by adding and removing a term to the Hamiltonian we can also control the state of a Carbon–13 atom. The Hamiltonian of the nuclear spin depends on the electronic spin state[12]. A hyperfine term describing the interaction between the electronic spin and the nucleus is not present when the electron is in the $m_s = 0$ state :

$$H_0 = \gamma_C B_z I_z \tag{3.1}$$

$$H_1 = \gamma_C B_z I_z + H_{\mathrm{HF}} \tag{3.2}$$

The hyperfine term consists of a contact term and a dipole term. For carbons with weak couplings (A<200kHz) the contact term is expected to be negligible and the dipole term is given by[3]:

$$H_{\mathrm{dip}} = \frac{\mu_0 \gamma_e \gamma_C \hbar^2}{4\pi r^3}[\boldsymbol{S}\cdot\boldsymbol{I} - 3(\boldsymbol{S}\cdot \hat{n_{\mathrm{hf}}})(\boldsymbol{I}\cdot \hat{n_{\mathrm{hf}}})] \tag{3.3}$$

From this equation the parallel and orthogonal components of the Hyperfine interaction ($H_{\mathrm{dip}} = A_{\parallel} I_z + A_{\perp} I_x$), with respect to the NV axis along the z direction, can be derived to be:

$$A_{\parallel} = -\frac{\mu_0 \gamma_e \gamma_C \hbar^2}{4\pi r^3}\left(3\cdot\frac{z^2}{r^2} - 1\right) \tag{3.4}$$

$$A_{\perp} = -\frac{\mu_0 \gamma_e \gamma_C \hbar^2}{4\pi r^3}\left(3\cdot\frac{\sqrt{x^2+y^2}\cdot z}{r^2}\right) \tag{3.5}$$

3.1 Addressing weakly-coupled carbons trough dynamical decoupling

Spins precess about a quantization axis along $\tilde{\boldsymbol{\omega}}$ with a frequency $|\tilde{\boldsymbol{\omega}}|$. We call $\tilde{\boldsymbol{\omega}}$ the quantization-vector. When the electron is in the $m_s = 0$ each nuclear spin precesses about $\tilde{\boldsymbol{\omega}} = \boldsymbol{\omega_L}$ with the Larmor frequency. The magnetic field is aligned along the quantization axis of the NV- center and defined as the z-direction.When the electron is in the $m_s = +1$ state nuclear spins precess about a distinct axis $\tilde{\boldsymbol{\omega}} = \boldsymbol{\omega_L} + \boldsymbol{A}$ [11]. The hyperfine interaction $\boldsymbol{A}$ depends on the position of that particular nuclear spin relative to the NV- center.

To understand how a Carbon–13 atom can be controlled it is useful to consider three situations. In the first situation the $\boldsymbol{\omega_L}$ and $\boldsymbol{A}$ point in the same direction. In the second situation $\boldsymbol{\omega_L}$ and $\boldsymbol{A}_{\perp}$ are of comparable magnitude, resulting in a large angle between the quantization axes. In the last situation $|\boldsymbol{A}|$ is small compared to $|\boldsymbol{\omega_L}|$ resulting in a small angle between the quantization axes.

When applying a decoupling sequence with N/2 decoupling units of the form $\tau-\pi-2\tau-\pi-\tau$, where τ is a wait time between pulses and π is a π-pulse that flips the electron-state, the nuclear spin alternately rotates around the $\boldsymbol{\omega}_L$ and the $\tilde{\boldsymbol{\omega}}$ axis. The net result of one such decoupling sequence is a rotation around an axis $\hat{\mathbf{n}}_{\mathbf{i}}$ by an angle ϕ. Where $\hat{\mathbf{n}}_{\mathbf{i}}$ depends on the initial state

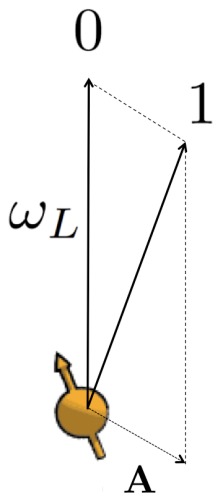

Figure 3.1 – Flipping the electron spin from the $m_s = 0$ to the $m_s = +1$ state changes the quantization axis of ^{13}C nuclear spins. For $m_s = 0$ spins precess about $\boldsymbol{\omega_L}$. For $m_s = +1$ spins precess about a distinct axis $\tilde{\boldsymbol{\omega}} = \boldsymbol{\omega_L} + \boldsymbol{A}$.

of the electron: $\hat{\mathbf{n_0}}$ when the electron starts in $m_s = 0$ and $\hat{\mathbf{n_1}}$ when the electron starts in $m_s = +1$ [11].

When $\boldsymbol{\omega_L}$ and $\boldsymbol{A}$ point in the same direction, the net rotation axis is independent of the initial electron-state making it impossible to use the electron to control the Carbon–13 atom using this decoupling sequence.

In the case where $\boldsymbol{\omega_L}$ and $\boldsymbol{A}_\perp$ are of comparable magnitude the net rotation axes $\hat{\mathbf{n_i}}$ are strongly dependent on the initial electron-state for almost any τ. Having one of these carbon atoms can make it hard to selectively control other carbons as there are very few inter-pulse-delays 2τ for which only the carbon atom without the strong orthogonal-hyperfine is affected.

When considering the case where $|\boldsymbol{A}|$ is small compared to $|\boldsymbol{\omega_L}|$ the net rotation axes $\hat{n_0}$ and $\hat{n_1}$ are practically parallel and the nuclear spin undergoes an unconditional evolution. Only when the inter-pulse delay is precisely resonant with the spin dynamics the axes are anti-parallel leading to a conditional rotation[11]. The resonant condition occurs at:

$$\tau = \frac{(2k+1)\pi}{2\gamma_C B_z + A_\parallel} \tag{3.6}$$

And for $\omega_L \gg |\boldsymbol{A}|$ the dip has a width of:

$$\Delta = \frac{A_\perp}{2 \cdot (\gamma_C B_z)^2} \tag{3.7}$$

If $\hat{n_0}$ and $\hat{n_1}$ are not parallel, the resulting conditional rotation of the nuclear spin generally entangles the electron and nuclear spins. As a result, for an unpolarized nuclear spin state, the final electron spin state is a statistical mixture of $|x\rangle$ and $|-x\rangle$ when starting from the $|x\rangle$ state. Where the probability that the initial state is preserved is given by:

$$P_x = (M+1)/2 \tag{3.8}$$

With for a single nuclear spin:

$$M = 1 - (1 - \hat{\mathbf{n_0}} \cdot \hat{\mathbf{n_1}}) \sin^2 \frac{N\phi}{2} \tag{3.9}$$

3.2 Characterizing the Nuclear-spin environment

In reality the electron is not interacting with a single carbon but with a bath of carbon atoms. When the electron interacts with multiple carbons at the same time the contrast M is given by the product of all individual values M_j for each individual spin j. In order to selectively control one carbon the electron should not entangle with any other carbon when addressing it.

To identify promising resonances for carbon control we perform a dynamical decoupling spectroscopy[11] or fingerprint. In a fingerprint experiment the electron is prepared in the

$|X\rangle = |0\rangle + |1\rangle$ state. It is subjected to a decoupling sequence consisting of N/2 blocks of the form $\tau - \pi - 2\tau - \pi - \tau$, and concluded by measuring $\langle X \rangle$. The fingerprint is the result of many repetitions for a range of inter-pulse delays 2τ. A narrow dip in the fingerprint spectrum is an indication a selectively controllable carbon.

By sweeping the number of π-pulses on such a dip it can be verified if it corresponds to a single carbon. If entanglement is created with a lot of spins at once all coherence is lost and contrast will go to 0. Only if no entanglement is created with any other carbon can the contrast be sweeped to -1.

Because Carbon-13 atoms are randomly distributed in diamond there is a wide range of possible hyperfine strengths. In the ideal case the spectrum would be filled with well-separated narrow resonances. This would correspond to carbons lying mostly along the NV-axis, ensuring weak orthogonal-components of the hyperfine interaction, and a decreasing density of carbon-13 atoms the further one goes away from the NV-center. Although such a distribution would not occur naturally this ideal case can be useful in understanding fingerprints.

Most carbon-spins have very similar hyperfine-interaction strengths as they are relatively far away from the NV-center. This causes their resonances to overlap manifesting itself as a broad feature with little coherence in the fingerprint. We identify this response as the spin-bath.

Spins that have a strong hyperfine-interaction relative to other spins show up outside or at the edge of the spin-bath response. Going to higher orders k separates resonances further allowing for control of more spins. As computations are fundamentally limited by the coherence time there is a limit to the resonance-order that can be used to address carbons. Additionally some of the relatively strong-coupled spins also have a strong orthogonal component of the hyperfine interaction. This orthogonal-component causes a broad response, effectively blocking a large range of τ from being used to control other spins.

Both these issues can be addressed by increasing the magnetic field. By increasing the magnetic field until the orthogonal hyperfine-components of all spins are small relative to the Larmor frequency the broad resonances that cause large parts of the spectrum to become useless disappear. Additionally all resonances move closer to $\tau = 0$ while at the same time becoming narrower, allowing higher order resonances to be addressed within the same coherence time.

Increasing the magnetic field will not always improve the situation. When the magnetic field is too strong the resonances become narrower than the resolution of the Arbitrary Waveform Generator used to generate the pulses that address these resonances, making it impossible to address them effectively. Similarly it is not practical to increase the magnetic field to compensate for arbitrary strongly coupled carbon-spins.

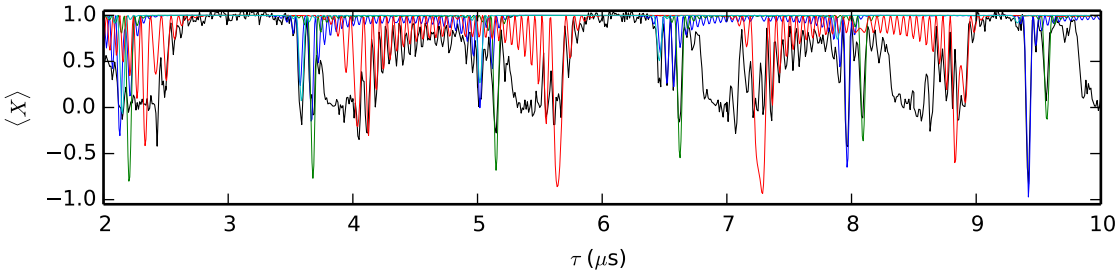

Figure 3.2 – Fingerprint of Hans Sil01 at B = 304.12G for N=32 pulses.Larmor revival clearly visible.

Carbon	$A_\parallel$	$A_\perp$
1	30.0 kHz·2π	80.0 kHz·2π
2	27.0 kHz·2π	28.5 kHz·2π
3	-51.0 kHz·2π	105.0 kHz·2π
4	45.1 kHz·2π	20.0 kHz·2π

Table 3.1 – Hyperfine paramters used to fit spins 1 to 4 in Figure 3.2.

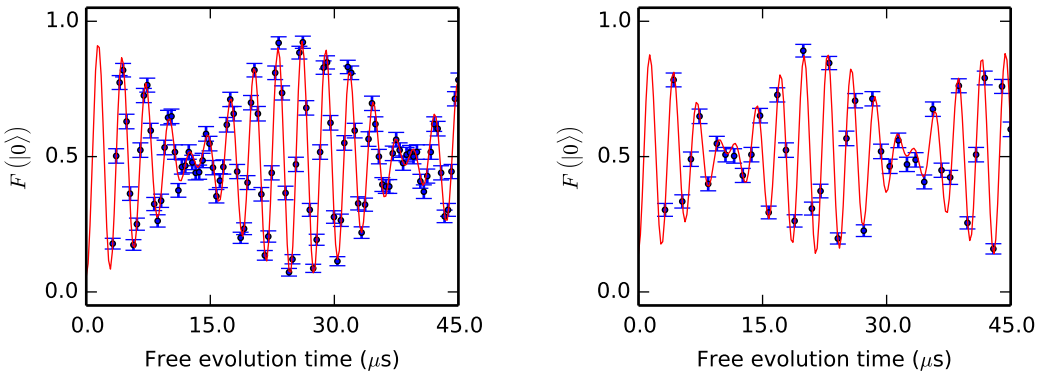

(a) Nuclear Ramsey of Carbon 1

(b) Nuclear Ramsey of Carbon 4

Figure 3.3 – Nuclear Ramsey experiment wit

3.3 Controlling weakly coupled carbons trough the electronic spin

3.4 Carbon Initialization & Readout

4

Deterministic Parity Measurements

4.1 Entanglement

4.2 Verification of Entanglement

5

Outlook: towards Quantum Error Correction

Lorem ipsum dolor sit amet, consectetur adipisicing elit, sed do eiusmod tempor incididunt ut labore et dolore magna aliqua. Ut enim ad minim veniam, quis nostrud exercitation ullamco laboris nisi ut aliquip ex ea commodo consequat. Duis aute irure dolor in reprehenderit in voluptate velit esse cillum dolore eu fugiat nulla pariatur. Excepteur sint occaecat cupidatat non proident, sunt in culpa qui officia deserunt mollit anim id est laborum.

Bibliography

[1] H. Bernien. *Control, Measurement and Entanglement of Remote Quantum Spin Registers in Diamond*. PhD thesis, Delft University of Technology, 2014.

[2] L. Childress and R. Hanson. Diamond nv centers for quantum computing and quantum networks. *MRS Bulletin*, 38(02):134–138, 2 2013. ISSN 0883-7694. URL http://www.journals.cambridge.org/abstract_S0883769413000201.

[3] G. de Lange. *Quantum Control and Coherence of Interacting Spins in Diamond*. PhD thesis, Delft University of Technology, 2012.

[4] M.W. Doherty, N.B. Manson, P. Delaney, F. Jelezko, J. Wrachtrup, and L.C.L. Hollenberg. The nitrogen-vacancy colour centre in diamond. page 101, 2 2013. URL http://arxiv.org/abs/1302.3288.

[5] Richard P. Feynman. Simulating physics with computers. *International Journal of Theoretical Physics*, 21(6-7):467–488, 6 1982. ISSN 0020-7748. URL http://link.springer.com/10.1007/BF02650179.

[6] F. Jelezko, T. Gaebel, I. Popa, a. Gruber, and J. Wrachtrup. Observation of coherent oscillations in a single electron spin. *Physical Review Letters*, 92(7):076401, 2 2004. ISSN 0031-9007. URL http://link.aps.org/doi/10.1103/PhysRevLett.92.076401.

[7] W. Pfaff. *Quantum Measurement and Entanglement of Spin Quantum Bits in Diamond*. PhD thesis, Delft University of Technology, 2013.

[8] L. Robledo, L. Childress, H. Bernien, B. Hensen, P.F.A. Alkemade, and R. Hanson. High-fidelity projective read-out of a solid-state spin quantum register. *Nature*, 477(7366):574–8, 9 2011. ISSN 1476-4687. URL http://www.ncbi.nlm.nih.gov/pubmed/21937989.

[9] P.W. Shor. Algorithms for quantum computation: discrete logarithms and factoring. In *Proceedings 35th Annual Symposium on Foundations of Computer Science*, pages 124–134. IEEE Comput. Soc. Press, 1994. ISBN 0-8186-6580-7. URL http://ieeexplore.ieee.org/lpdocs/epic03/wrapper.htm?arnumber=365700.

[10] T. H. Taminiau, J. J. T. Wagenaar, T. van der Sar, F. Jelezko, V. V. Dobrovitski, and R. Hanson. Detection and control of individual nuclear spins using a weakly coupled electron spin. *Physical Review Letters*, 109(13):137602, 9 2012. ISSN 0031-9007. URL http://link.aps.org/doi/10.1103/PhysRevLett.109.137602.

[11] T. H. Taminiau, J.J.T. J. T. Wagenaar, T. van der Sar, F. Jelezko, V.V. V. Dobrovitski, and R. Hanson. Detection and control of individual nuclear spins using a weakly coupled electron spin. *Physical Review Letters*, 109(13):137602, 9 2012. ISSN 0031-9007. URL http://arxiv.org/abs/1205.4128http://link.aps.org/doi/10.1103/PhysRevLett.109.137602.

[12] T. H. TH Taminiau, J. Cramer, T. van der Sar, V. V. Dobrovitski, and R. Hanson. Universal control and error correction in multi-qubit spin registers in diamond. *Nature Nanotechnology*, 2(February):2–7, 9 2014. ISSN 1748-3387. URL http://arxiv.org/abs/1309.5452http://www.nature.com/doifinder/10.1038/nnano.2014.2.

[13] L M Vandersypen, Matthias Steffen, Gregory Breyta, Costantino S Yannoni, Mark H Sherwood, and Isaac L Chuang. Experimental realization of shor's quantum factoring algorithm using nuclear magnetic resonance. *Nature*, 414(6866):883–7, 2001. ISSN 0028-0836. URL http://www.ncbi.nlm.nih.gov/pubmed/11780055.

A

State Initialization

B

Bell State Tomography

Derivation, what would a tomography of the Psi+ state look like?

C

Entanglement wittness

D

Simulations

Acknowledgements

Lorem ipsum dolor sit amet, consectetur adipisicing elit, sed do eiusmod tempor incididunt ut labore et dolore magna aliqua. Ut enim ad minim veniam, quis nostrud exercitation ullamco laboris nisi ut aliquip ex ea commodo consequat. Duis aute irure dolor in reprehenderit in voluptate velit esse cillum dolore eu fugiat nulla pariatur. Excepteur sint occaecat cupidatat non proident, sunt in culpa qui officia deserunt mollit anim id est laborum.